[Review Paper]

Synthesis of Nano-crystalline Zeolites and Applications to Zeolite Membranes

Teruoki TAGO*, Yuta NAKASAKA, and Takao MASUDA

Div. of Chemical Process Engineering, Faculty of Engineering, Hokkaido University, N13W8, Kita-ku, Sapporo 060-8628, JAPAN

(Received November 8, 2011)

The strong acidity and remarkable molecular sieving effect of zeolites makes them especially important materials in industrial reactions and separation processes. The use of zeolites as membranes combines the advantages of inorganic membranes (high temperature stability and solvent resistance) with the zeolitic properties. Such zeolite membranes have potential uses as separation and reaction membranes, and as simultaneous reaction/separation membranes. A number of approaches have proved effective for modifying the properties of zeolite membranes, including the use of nano-crystalline zeolites for membrane preparation, regioselective deactivation of acid sites, and modification of zeolitic pore size. This review describes the synthesis of nano-crystalline zeolites by an emulsion method and the regioselective deactivation of acid sites by the catalytic cracking of silane (CCS) method. The effects of the crystal size and CCS treatment on the performance of the zeolite membrane are reviewed.

Keywords

Nano-sized zeolite, Emulsion method, Catalytic cracking of silane, Zeolite membrane, Membrane reactor, Membrane separation

1. Introduction

Zeolites are crystalline aluminosilicate materials and possess intracrystalline pores and nanospaces of similar sizes to the molecules of the lighter hydrocarbons. Moreover, zeolites have strong acid sites on the nanopore surfaces within and on the external surfaces of the crystalline structure. These properties enable zeolites to be used as in reaction and separation processes, and these potential uses have led to the development of zeolite-based structured materials, such as zeolite films and membranes[1)~3)]. Zeolite membranes combine the properties of zeolites with those of inorganic membranes, so are attractive materials for various applications, such as selective reaction membranes[4),5)] and separation membranes[6)~9)]. ZSM-5 zeolite membranes were first prepared by Sano *et al.*[10),11)], and a great deal of subsequent research has focused on the use of zeolite membranes for reaction and separation.

To prepare a zeolite membrane by hydrothermal synthesis, zeolite seed crystals are deposited on a porous support, then secondary growth of the zeolite occurs to form the zeolite membrane. The uniformity of the membrane affects the reaction/separation properties, so the seeding of the zeolite crystals and the secondary growth process must occur uniformly[12)~16)]. Therefore, nano-sized zeolite crystals are expected to have good properties as seed crystals, because the smaller size allows for greater control of the seeding and growth processes. Mono-dispersed zeolite nanocrystals are expected to form uniform zeolite membranes.

This review describes a method for preparing nano-crystalline zeolites in a solution consisting of a surfactant, an organic solvent, and water (called the emulsion method[17)~21)]), and a method based on the catalytic cracking of silane[22)] (called the CCS method) for the regioselective deactivation of acid sites using silane compounds with various organic substituents. An MFI zeolite (ZSM-5) membrane was applied to the reaction of methanol to olefins[23),24)], to investigate the effect of the regioselective deactivation of acid sites by the CCS method on the olefin yields. A hydrophilic silicalite-1 membrane[25)] was prepared using silicalite-1 nanocrystals, to examine the effect of the crystal size on the separation properties[26),27)].

2. Synthesis of Nano-sized Zeolite Crystals

2. 1. Synthesis of Nano-crystalline Zeolites in Water/Surfactant/Organic Solvent

Zeolites are normally prepared in an aqueous alkaline solution containing Si and Al sources and alkaline metal ions (sodium or potassium). An organic structure directing agent (OSDA), such as an ammonium alkyl cation, is also necessary to form the zeolite framework in the synthesis of some types of zeolite. To prepare the zeolite, solutions containing these inorganic

* To whom correspondence should be addressed.
* E-mail: tago@eng.hokudai.ac.jp

materials and the OSDA are simply poured into a Teflon-sealed stainless bottle and heated to the required temperature.

Nano-crystalline zeolites can be prepared by quenching the hydrothermal treatment on nucleation. However, unreacted Si and Al species still remain in the solution, so an amorphous phase tends to form on the surface of the zeolite crystals. Another method involves increasing the nucleation rate by using higher concentrations of the Si and Al sources. By increasing the nucleation rate, the crystal size of the zeolite decreases. However, zeolites obtained by this method have a broad size distribution due to simultaneous nucleation and crystal growth during the hydrothermal treatment. Accordingly, it is important to separate the nucleation and growth stages to obtain nano-crystalline zeolite. Recently, nano-crystalline zeolites have been synthesized with the addition of surfactants, including in a water/surfactant/organic mixture[17)~21),28)~30)] (emulsion method). Research has focused on how to control the size and morphology of the crystals, because of the importance of these parameters in applications such as separation[26),27)] and catalytic reactions[31),32)]. Surfactant molecules have both hydrophobic and hydrophilic organic groups in the molecules, so adsorb onto the solid surface, thus reducing the interface energy difference between the solid surface and the solvent, and consequently enhancing nucleation of the metal and/or metal oxide nano-particles. Here, we describe the use of the emulsion method to prepare nano-crystalline zeolites.

In the emulsion method, two solutions are prepared; an aqueous solution containing the Si and Al sources diluted with an OSDA aqueous solution, and a solution of the surfactant in an organic solvent. Zeolite crystals with different properties can be prepared by varying the concentrations of the Si and Al sources in the aqueous solution, and the molar ratio of Si to OSDA, and by changing the type of OSDA. The aqueous solution is added to the surfactant organic solution, and the mixture is magnetically stirred at 323 K to obtain a homogeneous solution. The resulting mixture of water/surfactant/organic solvent is then placed in a Teflon-sealed stainless steel bottle, heated to 373 to 423 K, and held at the required temperature for 12 to 120 h with stirring to yield the nano-crystalline zeolites. In the emulsion method, two additional parameters are important; the concentration of surfactant in the organic solvent and the molar ratio of water to surfactant, because these parameters affect the morphology and crystal sizes.

2. 2. Effect of Ionicity of Surfactant on Preparation of Nano-crystalline Zeolites

The effect of the surfactant on the morphologies for MFI zeolite (silicalite-1) was examined using various surfactants at a hydrothermal temperature of 140 ℃ and a surfactant concentration in the organic solvent of 0.50 mol/L. In general, there are four types of surfactants; anionic, cationic, non-ionic, and bipolar surfactants. The present study used nonionic surfactants, polyoxyethylene(15)oleylether (O-15), polyoxyethylene(15)nonylphenylether (N-15), and poly(oxyethylene)(15)cethylether (C-15), and ionic surfactants, sodium bis(2-ethylhexyl) sulfosuccinate (AOT) and cetyltrimethyl ammonium bromide (CTAB). Cyclohexane or 1-hexanol was used as the organic solvent.

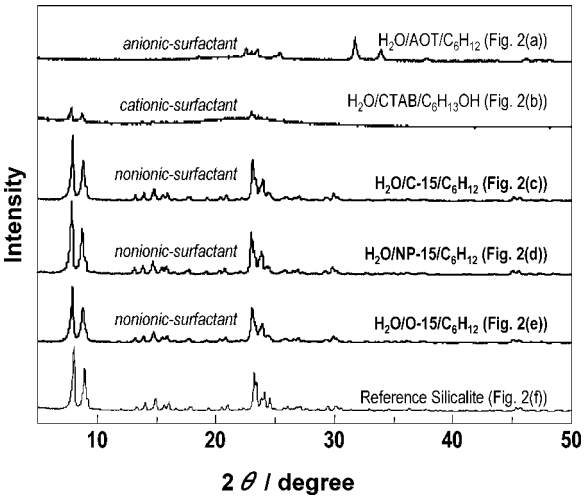

Effects of ionicity of the surfactant on the crystallinity of the MFI zeolite (silicalite-1).

Fig. 1 X-ray Diffraction Patterns of Samples Prepared in Water/Surfactant/Organic Solvent

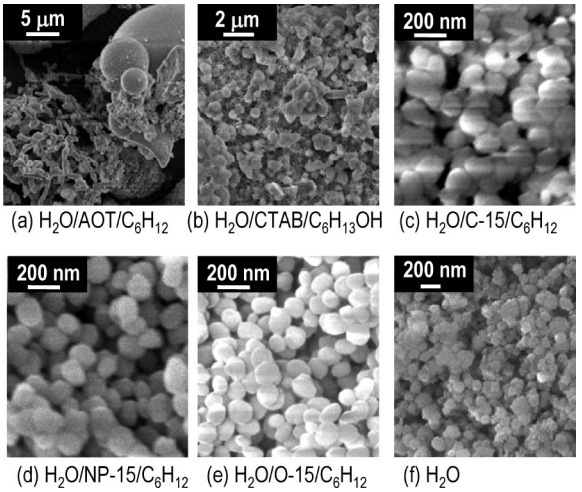

Effects of ionicity of the surfactant on the morphology of the MFI zeolite (silicalite-1). Si concentrations in water are (a)-(e) 0.63 mol/L and (f) 2.7 mol/L.

Fig. 2 FE-SEM Micrographs of Samples Prepared in Water/Surfactant/Organic Solvent

Figures 1 and **2** show the X-ray diffraction (XRD)

patterns and FE-SEM images of the obtained samples, respectively. For the sample prepared in the AOT/cyclohexane solution, the XRD pattern included peaks corresponding to sodium sulfate rather than silicalite-1. Moreover, the sample showed an irregular morphology. In this case, the tetra-*n*-propyl ammonium hydroxide (TPA^-OH) molecules did not act as an OSDA in the synthetic solution, possibly because the AOT surfactant and the TPA^-OH used as the OSDA have opposite ionic charges.

For the sample prepared in CTAB/1-hexanol, scanning electron microscope (SEM) showed silicalite-1 crystals of about 1.0 μm embedded in the amorphous SiO_2. XRD also showed the coexistence of silicalite-1 crystals and amorphous SiO_2. Since the pH of the synthetic solution is alkaline in this case, the surface of the SiO_2 had a negative charge. Accordingly, CTA^+ and TPA^+ were independently adsorbed on the surface of SiO_2 because of their cationic charges. Consequently, silicalite-1 crystals and amorphous SiO_2 were formed separately due to the independent adsorption of TPA^+ and CTA^+, respectively.

For the samples prepared in cyclohexane with the nonionic surfactants, C-15, NP-15, and O-15, XRD showed peaks corresponding to MFI zeolite (the reference silicalite-1), and SEM showed mono-dispersed silicalite-1 nanocrystals. In contrast, the silicalite-1 crystals prepared in water (without surfactant) had a heterogeneous structure and were present as smaller crystals (diameter of approximately 30 nm) formed on larger crystals (approximately 120 nm), indicating that nucleation, crystallization, and crystal growth occurred simultaneously. However, in the emulsion method, aggregation of the silicalite-1 nuclei is inhibited by the surfactants adsorbed on the surface during hydrothermal treatment, and mono-dispersed nanocrystals can be obtained. These results indicate that the ionicity of the hydrophilic groups in the surfactant molecules is important in the formation and crystallization processes of the nano-crystalline zeolites.

2. 3. Crystal Size Control

In the preparation of zeolite membranes, zeolite seed crystals are typically immobilized on porous supports before secondary growth. The crystallinity and the size of the zeolite seed crystals affect the secondary growth of the zeolite during membrane formation, so preparation of mono-dispersed zeolite nanocrystals is very important. In the emulsion method, adsorption of non-ionic surfactants on the surfaces of the zeolite precursors suppresses re-dissolution of the precursor in solution, thus inducing and enhancing nucleation of the zeolite. Control of the surfactant concentration is quite effective to suppress re-solution of the zeolite precursor. Accordingly, the effects of varying the O-15 surfactant concentration on the morphology of MFI (silicalite-1) and MOR zeolites were examined. **Figure 3** shows the FE-SEM images of the obtained samples. The Si/Al ratio of the MOR zeolites was 12.5. The surfactant concentrations were varied in the range from 0.5 to 0.75 mol/L, and preparation of zeolites from water solutions without surfactant/organic solvent (the conventional method) was also carried out for comparison. Interestingly, the crystal size and morphology depended on the surfactant concentration, despite use of the same concentrations of the Si, Al and OSDA throughout. Nano-crystalline zeolites with mean size of below 100 nm were obtained with a surfactant concentration of 0.5 mol/L. At higher concentrations, growth of MFI and MOR zeolites was clearly observed, with the crystal size reaching ～1.0 μm at 0.75 mol/L. The BET surface areas of the MFI and MOR zeolites were about 370 and 430 m^2/g, respectively, regardless of the crystal sizes[19),20),32)]. Moreover, temperature-programmed desorption (TPD) of the NH_3 profiles of the obtained MOR zeolites confirmed that these MOR zeolites with Si/Al ratio of 12.5 had almost the same acidity[32)].

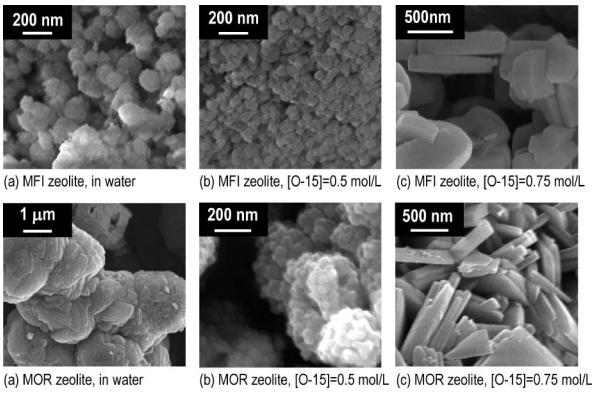

Fig. 3 FE-SEM Micrographs of MFI (silicalite-1) and MOR (Si/Al = 12.5) Zeolites with Different Crystal Sizes

3. Deactivation of Acid Site and Modification of Pore Size

3. 1. Catalytic Cracking of Silane Method

Because zeolites contain micropores of a specific diameter almost equal to the molecular sizes of the lighter hydrocarbons, they exhibit a remarkable molecular sieving effect for these hydrocarbons in reaction and adsorption processes, in which the spatial limitations within the zeolitic pores are expected to provide effective reaction/separation fields. Unfortunately, zeolites exhibit poor spatial limitation effects in some cases. For example, reactions over acid sites located on the external surface of the zeolite crystals can result in coke deposition, leading to a short catalyst lifetime. To overcome these problems, selective deactivation of acid sites located near the external surface of the zeolite crystal is required. Another problem occurs if all mol-

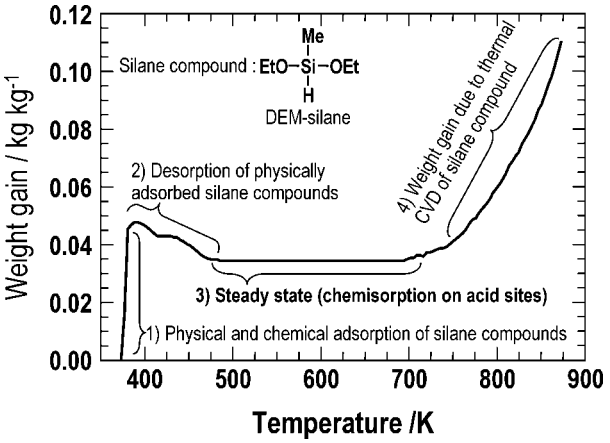

Fig. 4 Change in Weight Gain of MFI Zeolite in a Mixture of Silane Compound Vapor and N_2 Measured by Thermogravimetric Apparatus (heating rate: 5 K·min^{-1})

ecules have sizes smaller than the pore diameter. In this case, methods for modifying the pore wall and/or decreasing the pore size are needed for effective separation. Therefore, methods that allow regioselective deactivation and/or pore-size modification are required to improve the molecular sieving effect of zeolites.

Niwa *et al.*[33)~35)] have developed a method utilizing the chemical vapor deposition (CVD) technique with tetraethoxysilane and/or tetramethoxysilane precursors to form a thin silica (SiO_2) layer on the external surface of zeolite crystals. We have also proposed a method for SiO_2 formation based on the catalytic cracking of silane (the CCS method) using organic silane compounds, in which SiO_2 formation selectively occurs on the acid sites of the zeolite[22),32)]. The CCS method can use several types of silane compounds to deactivate the acid sites of zeolite, including silanes with methyl, ethoxy, and phenyl substituents. Because the molecular size of the silane compounds depends on the organic groups bonded to the Si atom, it is expected that selective deactivation of the acid sites located on the external surface of the zeolite crystals can be achieved by utilizing the molecular sieving effect of the zeolites to separate the silane compounds depending on their size[31)]. Moreover, if silane compounds smaller than the zeolite pores are used, SiO_2 formation may occur on the acid sites located on the pore surfaces within the crystals, leading to modification of the pore size[22)].

3. 2. Adsorption of Silane Compounds on MFI Zeolite

Figure 4 shows typical results for the weight changes observed during exposure of powdery MFI zeolite (proton-type ZSM-5, Si/Al = 15) to diethoxymethyl silane (DEM-Silane) vapor in a thermo-balance. A rapid weight increase was observed up to 400 K caused by chemisorption and physisorption of the silane compounds on the zeolite surface. The weight of the sample slightly decreased from 400 to 475 K, resulting from desorption of the physically adsorbed silane compounds on zeolite surface. No further weight changes were observed up to 700 K, indicating that the silane compounds chemisorbed on the acid sites reached an equilibrium state, which was confirmed by comparison of the number of adsorbed silane molecules with the number of acid sites of the zeolite[22)]. The weight of the zeolite rapidly increased above 700 K, due to thermal CVD and coke deposition by decomposition of the silane compounds.

In the CCS method, modification of the zeolite acidity and pore size can be achieved by SiO_2 unit formation, which occurs *via* a silane compound chemisorbed on the acid site of the zeolite. Accordingly, the procedure for the CCS method is outlined as follows[22),31),32)]. After air calcination, the zeolite is exposed to the silane compound vapor at 373 to 393 K in a N_2 stream, and the feed of the silane compound is then stopped to remove the physically adsorbed silane compounds on the zeolite surface. Therefore, the remaining silane compounds are chemisorbed on the acid sites of the zeolite. Next, the sample is heated to 823 K in a N_2 stream to decompose the silane compounds adsorbed on the acid sites, resulting in the formation of silicon-coke composites on the acid sites. Finally, the gas feed is switched from N_2 to air, and the temperature of the reactor is held at 823 K for 60 min, allowing the silicon-coke compounds formed on the acid sites to be oxidized to SiO_2 units. Therefore, the formation of SiO_2 units occurs on the acid sites which initially chemisorbed the silane compounds. By repeating this sequence, the formation of SiO_2 units occurs again on the acid sites, leading to decreases in the zeolite acidity and pore size.

3. 3. Regioselective Deactivation of Acid Sites by the CCS Method

The CCS method can use various silane compounds, such as diethoxymethylsilane (DEM-silane), phenylsilane (P-silane), diphenylsilane (DP-silane), diphenylmethylsilane (DPM-silane), and triphenylsilane (TP-silane). The order of the molecular sizes of the silane compounds is as follows (with the pore size of the MFI zeolite included for comparison); TP-silane$>$DPM-silane$\approx$DP-silane$\approx$pore diameter of MFI (10-membered rings)$>$P-silane$>$DEM-silane. With the phenylsilane compounds, the number of phenyl groups bonded to the Si atoms affects the molecular size of the silane compounds. **Figure 5** shows a schematic of the selective deactivation of acid sites by the CCS method, according to the molecular diameter of the precursor silane compounds. For organic silane compounds with almost the same molecular size as the pore size of the zeolite (*e.g.* DP-, DPM- and TP-silanes), selective deactivation occurs at acid sites located near the external surface of the MFI zeolite (ZSM-5) crystal. In contrast, for silane compounds with molecular sizes smaller than the

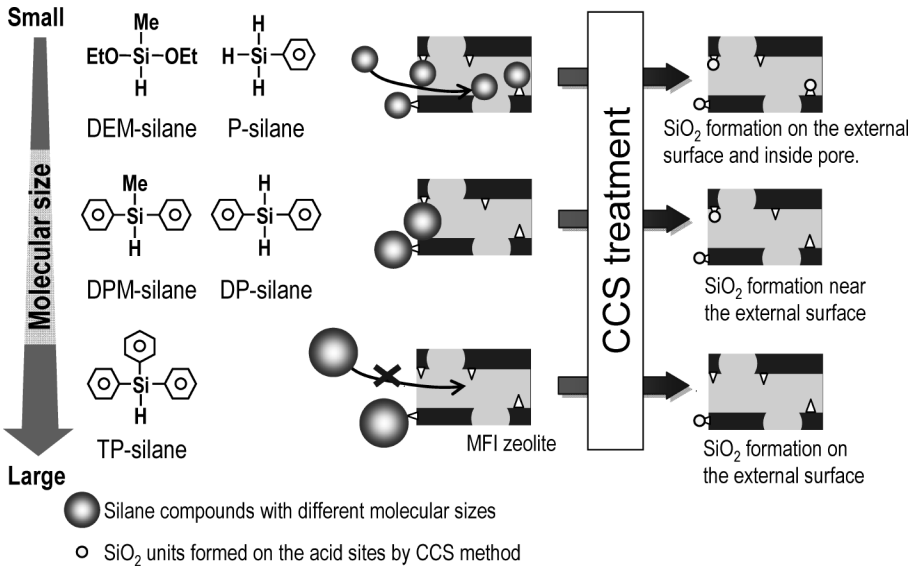

Fig. 5 Schematic Showing the Relationship between the Molecular Sizes of the Precursor Silane Compounds and the Regioselective Deactivation of Acid Sites by the CCS Method

pore size of the zeolite (*e.g.* P-silane and DEM-silane), acid sites are accessible on the pore surfaces within the crystal as well as near the external surface, enabling modification of the pore size. As a result, different distributions of acid sites on the MFI zeolite (ZSM-5) can be achieved by regioselective deactivation using silane compounds with different molecular sizes.

4. Applications of Zeolite Membrane for Gas-phase Reaction/Separation

4. 1. Experimental Apparatus for Gas-phase Reaction/Separation Using Zeolite Membrane

Zeolite membranes have been applied to simultaneous reaction and separation systems[5),36)~38)]. These zeolite membrane reactors can be divided into two configurations: catalyst placed on top of a zeolite layer[39)~41)], and homogeneous membranes containing zeolite crystals[42)~47)]. Zeolite membrane reactors based on a catalytic zeolite layer are less common[36),48),49)]. In such a reactor, molecules are transported to the external surface of the zeolite layer and penetrate into the layer, then react over the active sites of the zeolite. The reactions cease after the molecules have passed through the layer.

In the present study, an MFI zeolite (ZSM-5) membrane was prepared by forming a MFI zeolite layer on the surface of a cylindrical porous alumina ceramic filter with an inner diameter of 6 mm, an outer diameter of 11 mm, and a length of 50 mm. The filter pores had a diameter of 0.1 μm. Three reactant solutions were mixed for the hydrothermal preparation of the MFI zeolite membrane: sodium chloride solution, sodium silicate solution and aluminum sulfate solution containing tetra-*n*-propyl ammonium bromide (TPABr). The alumina ceramic filter with seed MFI zeolite crystals (ZSM-5 with crystal size of about 1000 nm) was immersed into the mixture followed by hydrothermal treatment to form the MFI zeolite membrane on the surface of the filter. After ion-exchange treatment from Na^+ to NH^{4+} and air calcination to remove the TPABr molecules, the membrane was used in further experiments.

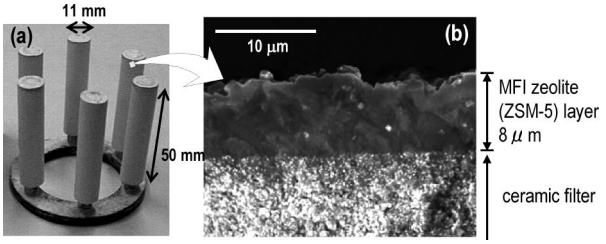

Fig. 6 (a) Overview and (b) Cross-sectional Area of the Prepared Membrane (ZSM-5 membrane)

Figure 6 shows the overview and cross-sectional area of the prepared membrane (ZSM-5 zeolite layer with Si/Al ratio of 15). XRD showed that the membrane layer had the same structure as MFI zeolite, indicating that the zeolite membrane consisted of MFI zeolite (ZSM-5)[22),23)]. Moreover, the zeolite layer formed on the outer surface of the alumina ceramic filter was dense and uniform. Applications of zeolite membrane to gas-phase separation and reaction require a dense membrane without physical holes for optimum separation properties of gaseous molecules, based on the molecular sieving effect of the micropore of the zeolite. Accordingly, the dense membrane shown in **Fig. 6** was

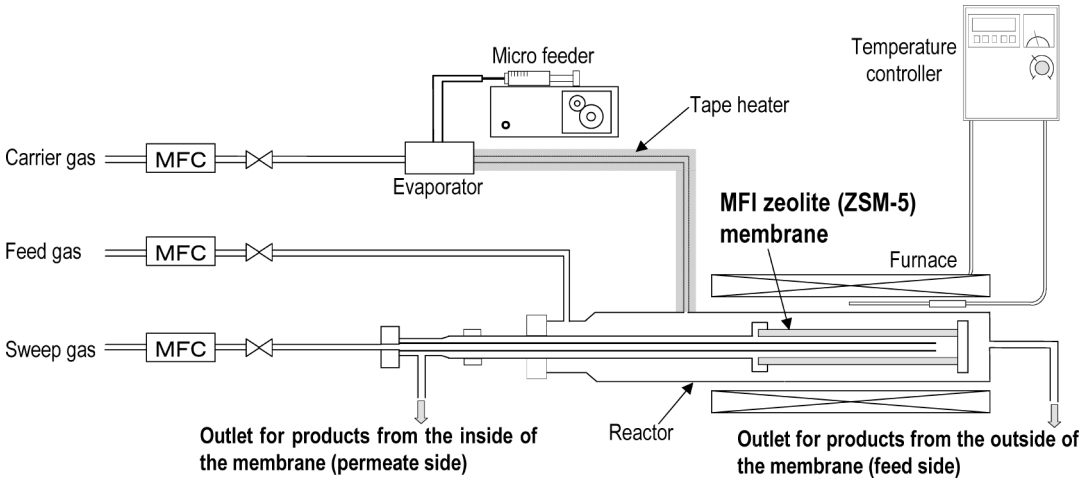

Fig. 7 Schematic of the MFI Zeolite Membrane Reactor/Separator for Gas Phase Applications

suitable for further applications.

Figure 7 shows a schematic view of the apparatus used for gas-phase reaction/separation in a flow system. One end of the cylindrical zeolite membrane was sealed, and a gas mixture of H_2 and N_2 (for gas separation) or methanol and N_2 (for reaction) were fed to the outer side (feed side) of the membrane. Helium (He) or N_2 gas was fed to the sealed end of the membrane from a pipe inserted in the inner side (permeate side of the membrane) of the sample holder to allow backflow to sweep out the permeating molecules. The gas compositions in the feed and permeate sides were measured using a quadrupole mass analyzer and gas chromatography (GC-8A, Shimadzu Corp., Japan).

4. 2. MTO Reaction Using MFI Zeolite Membrane Treated by the CCS Method

This study showed that SiO_2 units are selectively formed on the acid sites of the zeolite by the CCS method. Moreover, regioselective deactivation of acid sites can be achieved by the CCS method using silane compounds with different molecular sizes. Next, the methanol to olefins reaction (MTO reaction) was investigated using the MFI zeolite (ZSM-5) catalytic membrane to assess the effect of CCS treatment on the product yields of MTO reaction.

The MTO reaction using the catalytic zeolite membrane was expected to form light olefins such as ethylene and propylene followed formation of paraffins and aromatics at the feed side of the membrane, due to the nonshape-selective reactions over the acid sites of the membrane facing the feed side. In order to increase the olefin yield, such nonshape-selective reactions must be limited without any reduction in olefin formation. For this purpose, regioselective deactivation of the acid sites by the CCS method may be achieved using silane compounds with larger molecular sizes than the pore size of the zeolite, providing selective deactivation at acid sites located on and/or near the external surface.

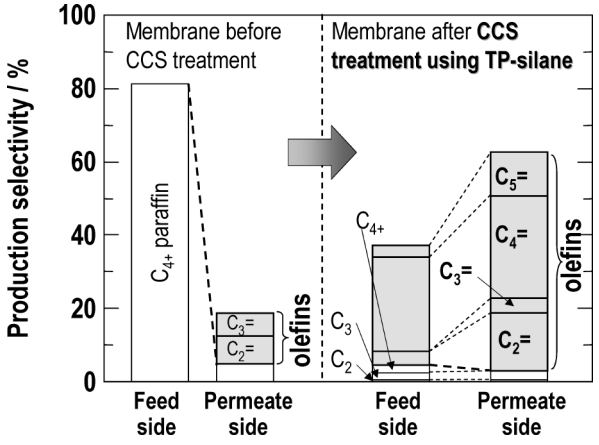

Fig. 8 Product Selectivities Obtained from the Feed and Permeate Sides of the Membrane during the MTO Reaction

In this study, selective deactivation of the acid sites on the external surface of the zeolite membrane was achieved without deactivation of acid sites in the zeolite pores in an attempt to increase the olefin yields. **Figure 8** shows the typical production selectivity for the MTO reaction using the ZSM-5 zeolite membranes before and after CCS treatment using TP-silane. Membranes before CCS treatment formed olefins in the products recovered from the permeate side, but the selectivity for paraffins at the feed side was much higher than the selectivity for olefins at the permeate side. Paraffin production at the feed side resulted from the conversion of methanol to paraffins over acid sites on the external surface of the membrane facing the feed side. Moreover, the paraffins formed at the feed side had longer chain lengths than the olefins and paraffins formed at the permeate side. These longer chain products result from the nonshape-selective reactions of the hydrocarbons over the acid sites on the surface of the membrane facing the feed side. In contrast, the zeolite

membrane after CCS treatment using TP-silane showed markedly reduced selectivity for paraffins at both the feed and permeate sides. Moreover, the olefin selectivity at the permeate side was higher than that at the feed side. The acid sites on the surface facing the feed side of the zeolite membrane were selectively deactivated by the CCS method using TP-silane, so suppressing the formation of undesirable products through reactions with ethanol, such as paraffins and aromatics.

4. 3. H_2 Separation Using MFI Zeolite Membrane Treated by the CCS Method

The MFI zeolite (ZSM-5) membrane treated by the CCS method was applied to the separation of H_2 from mixtures of gases containing H_2 and N_2 or O_2. The experimental apparatus shown in **Fig. 6** was also applied for the gas-phase separations. All molecules permeating from the feed side to the permeate side of the membrane must pass through the pores of the MFI zeolite. The CCS method using DEM-silane and P-silane, which are smaller than the pore size of the zeolite, is expected to form SiO_2 units on acid sites inside the pores of the crystal as well as on the external surface. Accordingly, the pore sizes of the MFI zeolite (ZSM-5) are decreased to a size only slightly larger than the molecular sizes of N_2 and O_2, but significantly larger than that of H_2. Therefore, the diffusion rate ratio of H_2 to N_2 or H_2 to O_2 through the membrane is expected to be greater for the MFI zeolite membrane after CCS treatment than for the membrane before CCS treatment.

Figure 9 shows the overall mass transfer coefficient of the membrane (permeance) for H_2 at different molar fractions for a mixture of H_2 and N_2 at the feed side. To investigate the gas-separation behavior, MFI zeolite (ZSM-5) membranes before and after CCS treatment using DEM-silane were used. Over a wide range of H_2 molar fractions, the permeance of N_2 decreased markedly (to about 1/500) for the membrane after CCS treatment, whereas that of H_2 was much less decreased (to about 1/10). Based on the measured permeances and molar fractions of H_2 and N_2 at the feed and permeate sides, the separation factor for H_2 was calculated as 90 to 140 for the treated membrane, or about 50 times greater than that of the original membrane (1.5-4.5). Similar results were obtained for mixtures of H_2 and O_2 (H_2 separation factor of 110-120). The kinetic diameters of H_2, N_2, O_2, and CO_2 are 0.28, 0.36, 0.33 and 0.33 nm, respectively. The diameter of a silicon cation with a coordination number of 4 is about 0.08 nm, whereas the pore diameter of the MFI zeolite is about 0.55 nm. Therefore, the pore size at locations where SiO_2 has formed is considered to be in the range of $\sim$0.47 nm (= 0.55 nm-0.08 nm). Consequently, the SiO_2 formed by the CCS method can reduce the pore size of the zeolite, enabling better gas separation.

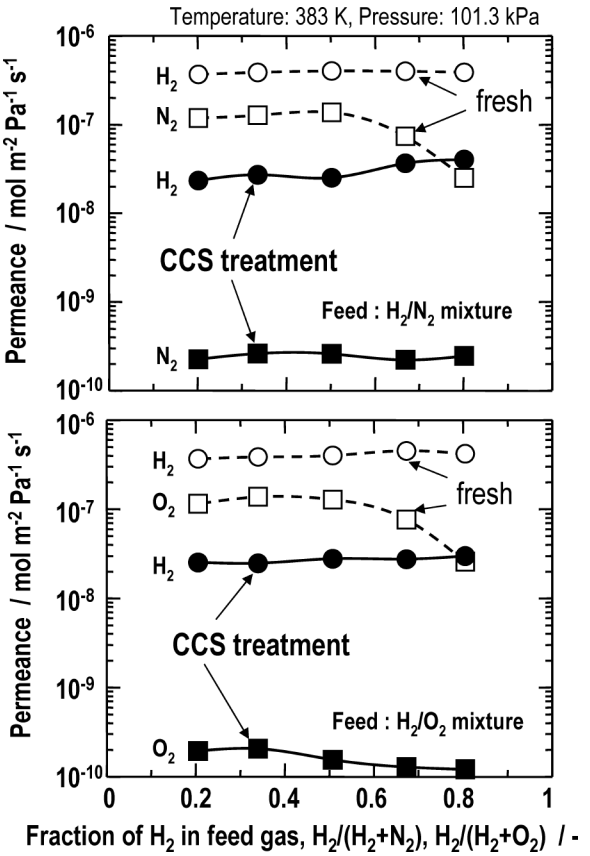

Fig. 9 Permeances of MFI Zeolite Membranes for H_2, N_2, and O_2 in a Flow System Using Different Molar Fractions of H_2 in the Feed Gas

5. Applications of Zeolite Membrane for Liquid-phase Separation

5. 1. Pervaporation Membrane

Separation and purification processes of liquid mixtures are among the most important unit-operations in the petrochemical industry, and are primarily carried out using distillation columns. However, the distillation process requires huge amounts of energy due to the large number of plates in the distillation columns and the high reflux ratio, which is above 20. Accordingly, alternative methods for high purity separation are necessary, with pervaporation emerging as a promising solution.

In the pervaporation method, the feed liquid mixtures are contacted with one side of a membrane (feed side), and the target components are removed from the mixture as vapor from the other side of the membrane (permeate side) after permeation through the membrane. The relative affinities (*e.g.* hydrophilic or hydrophobic interaction) between the membrane and the various components in the liquid solution allow for selective permeation that is superior to the separation obtained by distillation, which relies on the vapor-liquid equilib-

rium. Therefore, several types of zeolite membranes have been prepared and studied as potential pervaporation membranes for dehydration of organic solvents such as ethanol, isopropanol, and acetone[50)~55)], due to the high stabilities at high temperatures and strong resistance to organic solvents. The function of zeolite membranes to perform selective dehydration by pervaporation depends on the hydrophilic properties, which in turn depend on the composition of elements within the constituent components, such as the Si/Al ratio. However, dealumination may occur in acid solutions with zeolites containing Al_2O_3, resulting in reduction in the separation factor due to the generation of defects after long-term use. Therefore, Al_2O_3-free zeolite membranes should be used for such applications.

5. 2. Preparation of Hydrophilic and Al_2O_3-free Zeolite Membrane

Silicalite-1, which has an MFI structure, is a suitable Al_2O_3-free zeolites with the potential to avoids generation of defects caused by dealumination. Prepared MFI zeolites are usually calcined in air at 803 K, to remove any OSDA molecules from within the zeolite. However, during this procedure, silanol groups undergo dehydration to form siloxane bonds, resulting in a hydrophobic surface. Accordingly, the preparation of hydrophilic silicalite-1 membranes is not well characterized. To prepare silicalite-1 membrane with high hydrolytic properties retaining the silanol groups, we have proposed a liquid phase oxidation technique[25)~27)] by modifying the method reported by Fukuoka[56)]. Briefly, silicalite-1 membranes prepared without air calcination were immersed into a nitric acid solution (300 cm^3, 1 mol/L) and the solution heated to a reflux condition. Then, hydrogen peroxide solution (30 cm^3, H_2O_2, 30 wt%) was slowly added to the solution, and maintained for 24 h under reflux. The treated membrane was washed by distilled water, dried under an air stream, and then used in the experiments.

The silicalite-1 membranes obtained after liquid-phase oxidation using H_2O_2 retain considerable numbers of hydrophilic silanol groups on the silicalite-1 surface, to which water molecules selectively adsorb. Moreover, the water–silanol bonding networks that form on the non-zeolitic pores of the silicalite-1 crystals are the dominant channels for permeation of water molecules, allowing water molecules to selectively diffuse through the network, resulting in a high separation factor (**Fig. 10**). As the size of the crystals decreases, the number of hydrophilic channels for water permeation is expected to increase, leading to improvement of the water flux in addition to the separation factor. Accordingly, membranes were prepared using nanocrystalline silicalite-1 with different crystal sizes, and the effect of the crystal sizes on the separation of water from water–acetone solution was examined.

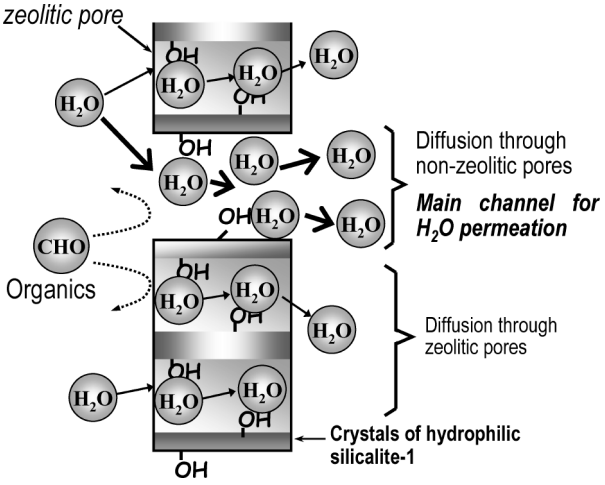

Possible relationships between the water molecules and silanol groups allowing formation of channels for water permeation.

Fig. 10 Mechanisms for Selective Permeation of Water through Hydrophilic Silicalite-1 Membrane

5. 3. Hydrophilic Silicalite-1 Membrane

Silicalite-1 nanocrystals were ultrasonically dispersed in alkaline water solution at a pH of approximately 10. The dispersed nanocrystals were layered on the outer surface of a cylindrical alumina ceramic filter (as described in section **4. 1.**) by a filtration method with evacuation on the inner side. The thickness of the silicalite-1 nanocrystal layer deposited on the ceramic filter could be controlled by changing the concentration of the silicalite-1 nanocrystal in the water solution. Finally, a silicalite-1 layer (protective layer) was hydrothermally formed on the nanocrystal layer, as described previously[26),27)].

Figures 11(a) and **11(b)** show SEM micrographs of the cross-sectional area and top view, respectively, of the silicalite-1 nanocrystal-layered membrane. The nano-crystalline silicalite-1 used for the preparation of the membrane had a crystal diameter of 60 nm. The nanocrystalline layer with a thickness of approximately 4.0 μm could be clearly observed on the alumina filter, together with a protective layer of columnar crystalline silicalite-1 with a thickness of approximately 1.2 μm on top of the nanocrystal layer. As shown in **Fig. 11(b)**, many large pores can be observed among the silicalite-1 crystals of the protective layer. The crystalline size in the protective layer was approximately 1000 nm, and was much bigger than that of the nano-crystalline silicalite-1. The morphology of the top view suggests that the protective layer had almost no separation function. In contrast, secondary growth of the nanocrystals can be observed around the interface between the protective and nanocrystalline layers. Such growth of nanocrystals occurred during the formation of the protective layer. Pera-Titus *et al.*[14)], and Hasegawa *et*

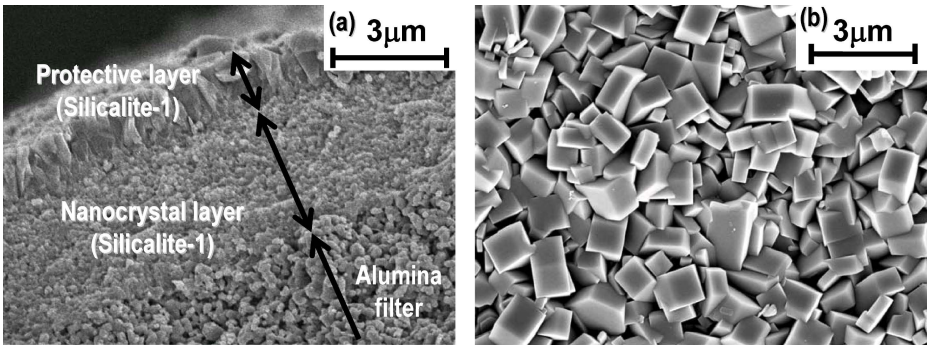

Fig. 11 SEM Images of (a) Cross-section and (b) Top View of the Silicalite-1 Nanocrystal-layered Membrane

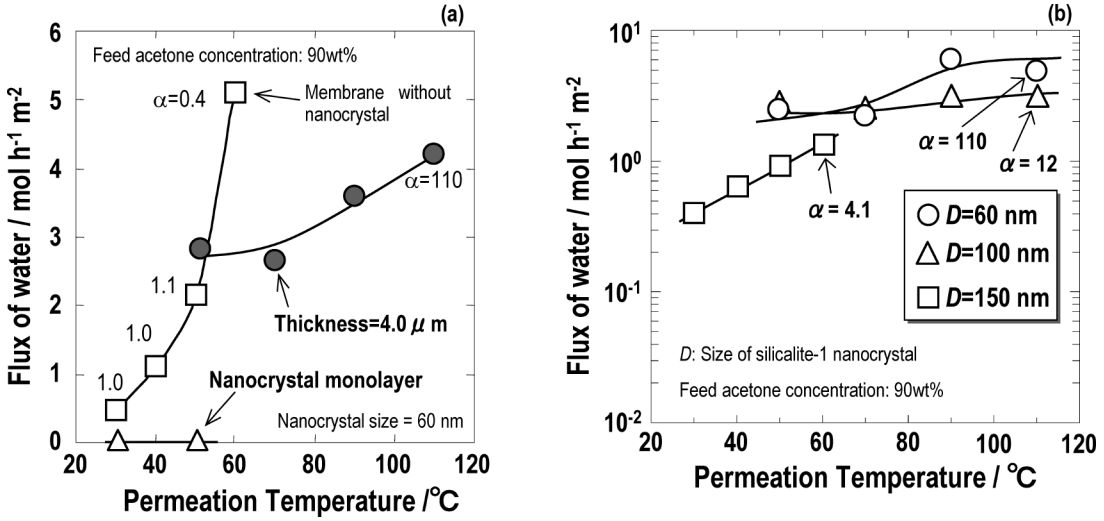

The acetone concentration was 90 wt%.

Fig. 12 Effects of (a) Layer Thickness of and (b) Crystal Size of Nano-crystalline Silicalite-1 on the Water Flux through the Layered Membrane

al.[15),16)] have reported that the amount of seed crystals on the support affected the secondary growth of seed crystals and the membrane characteristics for pervaporation and gas separation. Therefore, the effect of the thickness of the nanocrystalline layer on the separation properties was investigated.

The thicknesses were a 60 nm for the nanocrystal monolayer and 4.0 μm for the nanocrystal layer, and after depositing the nanocrystals, the silicalite-1 protective layer was formed at a hydrothermal temperature of 140 ℃. **Figure 12(a)** shows the effects of the thickness of the nanocrystal layer on the separation of water through the layered membrane. In the membrane prepared without the nanocrystal layer, the silicalite-1 protective layer was directly formed on the alumina filter by hydrothermal synthesis. This membrane without the nanocrystal layer showed no separation function, indicating that the silicalite-1 nanocrystal layer was essential for the separation function. In the membrane with a nanocrystal monolayer, excessive secondary growth of the nanocrystals had occurred, leading to formation of a dense silicalite-1 layer, so that both water and acetone molecules could not permeate the membrane. In contrast, in the membrane with a nanocrystal layer of 4.0 μm thickness, appropriate pores for selective permeation of water were formed among the nanocrystals by secondary growth, so that the membrane exhibited high water flux with high separation factor.

The dependency of the separation performance on the amount of silicalite-1 nanocrystals was ascribed to the secondary growth during hydrothermal synthesis to form the protective layer[27)], which was in good agreement with the previous reports[14)~16)], and since the protective layer was formed by secondary growth of the silicalite-1 nanocrystals in the layer, the active separation region was considered to be the interface between the nanocrystal and protective layers. Zeolite mem-

branes formed on porous ceramic filters in this way usually suffer from the serious problem of thermal mismatch caused by the different expansion coefficients of the zeolite layer and the alumina filter. In contrast, the thick nanocrystal layer on the alumina filter compensates for this mismatch because the active separation region is located at the interface between the nanocrystal and protective layers.

Figure 12(b) shows the effects of the crystal size of the nano-crystalline silicalite-1 on the separation of water from a water–acetone solution passed through the layered membranes, where D and α represent the crystal size and the separation factor, respectively. The flux of water through the layered membranes increased with higher permeation temperature. Decreased crystal sizes of the silicalite-1 resulted in dramatically increased water flux as well as separation factor, which was considered to result from reduction in the mesopore spaces between the initial crystals and the spaces remaining after secondary growth. Accordingly, the separation factor increased with smaller crystal size of the nano-crystalline silicalite-1. Moreover, the decrease in crystal size also caused higher numbers of hydrophilic channels between the crystals, allowing the water flux to increase through the channels of water–silanol networks for the selective permeation of water molecules.

6. Conclusion

Reaction and separation processes are very important petrochemical processes, for which zeolites are used widely as catalysts and adsorbents. The surface properties of zeolite crystals can be easily modified by post-synthesis treatments such as ion-exchange and using organic silane compounds, so zeolites are expected to be useful in a wide range of new applications. One promising application is the use of zeolites in membranes, which combine the properties of zeolites with those of inorganic membranes. The present review introduces the use of nano-crystalline zeolites in membrane preparation, and modification of the acid sites and pore sizes of the zeolite membranes. The size-controlled synthesis of nano-zeolites was achieved by an emulsion method, and reduction in crystal size led to improved separation properties for a pervaporation membrane. The CCS method could be used to selectively deactivate acid sites located on the feed side of the zeolite membrane. The membrane treated by the CCS method exhibited high olefin selectivity in an MTO reaction. The use of nano-crystalline zeolites and regioselective deactivation of the acid sites in the zeolite membrane are effective for controlling the zeolite properties in a membrane configuration.

Acknowledgment

This work was partly supported by the Research Grant Program from the New Energy and Industrial Technology Development Organization (NEDO) of Japan.

References

1) Bein, T., *Chem. Mater.*, **8**, 1636 (1996).
2) Tavolaro, A., Drioli, E., *Adv. Mater.*, **11**, (12), 975 (1999).
3) Caro, J., Noack, M., Kolsch, P., Schafer, R., *Micropor. Mesopor. Mater.*, **38**, 3 (2000).
4) Igarashi, H., Uchida, H., Suzuki, M., Sasaki, Y., Watanabe, M., *Appl. Catal. A: General*, **159**, 159 (1997).
5) Hasegawa, Y., Kusakabe, K., Morooka, S., *J. Membr. Sci.*, **190**, 1 (2001).
6) Kita, H., Horii, K., Ohtoshi, Y., Tanaka, K., Okamoto, K., *J. Mat. Sci. Lett.*, **14**, 206 (1995).
7) Bakker, W. J. W., Kapteijn, F., Poppe, J., Moulijn, J. A., *J. Membr. Sci.*, **117**, 57 (1996).
8) Kondo, M., Komori, M., Kita, H., Okamoto, K., *J. Membr. Sci.*, **133**, 133 (1997).
9) Kusakabe, K., Kuroda, T., Murata, A., Morooka, S., *Ind. Eng. Chem. Res.*, **36**, 649 (1997).
10) Sano, T., Kiyozumi, Y., Kawamura, M., Mizukami, F., Takaya, H., Mouri, T., Inaoka, W., Toida, Y., Watanabe, M., Toyoda, K., *Zeolite*, **11**, 842 (1991).
11) Sano, T., Yanagishita, H., Kiyozumi, Y., Mizukami, F., Haraya, K., *J. Membr. Sci.*, **95**, 221 (1994).
12) Masuda, T., Hara, H., Kouno, M., Kinoshita, H., Hashimoto, K., *Micropor. Mesopor. Mat.*, **3**, 565 (1995).
13) Masuda, T., Sato, A., Hara, H., Kouno, M., Hashimoto, K., *Appl. Catal. A: General*, **111**, 143 (1994).
14) Pera-Titus, M., Llorens, J., Gunill, F., Mallada, R., Santamaria, J., *Catal. Today*, **104**, 281 (2005).
15) Hasegawa, Y., Ikeda, T., Nagase, T., Kiyozumi, Y., Hanaoka, T., Mizukami, F., *J. Membr. Sci.*, **280**, 397 (2006).
16) Hasegawa, Y., Nagase, T., Kiyozumi, Y., Mizukami, F., *J. Membr. Sci.*, **294**, 186 (2007).
17) Tago, T., Nishi, M., Kouno, Y., Masuda, T., *Chem. Lett.*, **33**, 1040 (2004).
18) Tago, T., Iwakai, K., Nishi, M., Masuda, T., *Stud. Surf. Sci. Catal.*, **159**, 185 (2006).
19) Tago, T., Iwakai, K., Nishi, M., Masuda, T., *J. Nanosci. Nanotechnol.*, **9**, 612 (2009).
20) Tago, T., Aoki, D., Iwakai, K., Masuda, T., *Top. Catal.*, **52**, 865 (2009).
21) Iwakai, K., Tago, T., Konno, H., Nakasaka, Y., Masuda, T., *Micropor. Mesopor. Mat.*, **141**, 167 (2011).
22) Masuda, T., Fukumoto, N., Kitamura, M., Mukai, S. R., Hashimoto, K., Tanaka, T., Funabiki, T., *Micropor. Mesopor. Mat.*, **48**, 239 (2001).
23) Masuda, T., Asanuma, T., Shouji, M., Mukai, S. R., Kawase, M., Hashimoto, K., *Chem. Eng. Sci.*, **58**, 649 (2003).
24) Tago, T., Iwakai, K., Morita, K., Tanaka, T., Masuda, T., *Catal. Today*, **105**, 662 (2005).
25) Masuda, T., Otani, S., Tsuji, T., Kitamura, M., Mukai, S. R., *Separ. Purif. Tecnol.*, **32**, 181 (2003).
26) Tago, T., Nakasaka, Y., Kayouda, A., Masuda, T., *Separ. Purif. Tecnol.*, **58**, 7 (2007).
27) Tago, T., Nakasaka, Y., Kayouda, A., Masuda, T., *Micropor. Mesopor. Mat.*, **115**, 176 (2008).
28) Kuechl, D. E., Benin, A. I., Knight, L. M., Abrevaya, H., Wilson, S. T., Sinkler, W., Mezza, T. M., Willis, R. R., *Micropor. Mesopor. Mat.*, **127**, 104 (2010).

29) Naik, S. P., Chen, J. C., Chiang, A. S. T., *Micropor. Mesopor. Mat.*, **54**, 293 (2002).
30) Lee, S., Carr, C. S., Shantz, D. F., *Langmuir*, **21**, 12031 (2005).
31) Tago, T., Sakamoto, M., Iwakai, K., Nishihara, H., Mukai, S. R., Tanaka, T., Masuda, T., *J. Chem. Eng. Jpn.*, **42**, 162 (2009).
32) Tago, T., Konno, H., Sakamoto, M., Nakasaka, Y., Masuda, T., *Appl. Catal. A: General*, **403**, 183 (2011).
33) Niwa, M., Murakami, Y., *J. Phys. Chem. Sol.*, **50**, 487 (1989).
34) Niwa, M., Yamazaki, K., Murakami, Y., *Ind. Eng. Chem. Res.*, **30**, 38 (1991).
35) Katada, N., Niwa, M., *Chem. Vap. Dep.*, **2**, 125 (1996).
36) Armor, J. N., *Catal. Today*, **25**, 199 (1995).
37) Hasegawa, Y., Sotowa, K., Kusakabe, K., Morooka, S., *Micropor. Mesopor. Mat.*, **53**, 37 (2002).
38) McLeary, E. E., Jansen, J. C., Kapteijn, F., *Micropor. Mesopor. Mat.*, **90**, 198 (2006).
39) Van der Puil, N., Rodenburg, E. C., van Bekkum, H., Jansen, J. C., *Stud. Surf. Sci. Catal.*, **97**, 377 (1995).
40) Tanaka, K., Yoshikawa, R., Ying, C., Kita, H., Okamoto, K., *Catal. Today*, **67**, 121 (2001).
41) Liu, B. S., Gao, L. Z., Au, C. T., *Appl. Catal. A: General*, **235**, 193 (2002).
42) Parton, R. F., Vankelecom, I. F. J., Casselman, M. J. A., Bezoukhanova, C. P., Uytterhoeven, J. B., Jacobs, P. A., *Nature*, **370**, 541 (1994).
43) Cot, L., Ayral, A., Durand, J., Guizard, C., Novnanian, N., Julbe, A., Larbot, A., *Solid State Sci.*, **2**, 313 (2000).
44) Lin, Y. S., *Separ. Purif. Technol.*, **25**, 39 (2001).
45) Wu, S. Q., Gallot, J. E., Bousmina, M., Bouchard, C., Kaliaguine, S., *Catal. Today*, **56**, 113 (2000).
46) Langhendries, G., Baron, G. V., *J. Membr. Sci.*, **141**, 265 (1998).
47) Vital, J., Ramos, A. M., Silva, I. F., Castanheiro, J. E., *Catal. Today*, **67**, 217 (2001).
48) Antia, J. E., Govind, R., *Ind. Eng. Chem. Res.*, **34**, 140 (1995).
49) Tuan, V. A., Li, S. G., Falconer, J. L., Noble, R. D., *Chem. Mater.*, **14**, 489 (2002).
50) Matsukata, M., Kikuchi, E., *Bull. Chem. Soc. Jpn.*, **70**, 2341 (1997).
51) Mizukami, F., *Stud. Surf. Sci. Catal.*, **125**, 1 (1999).
52) Noack, M., Kolsch, P., Caro, J., Schneider, M., Toussaint, P., Sieber, I., *Micropor. Mat.*, **35**, 253 (2000).
53) Lin, X., Kikuchi, E., Matsukata, M., *Chem. Commun.*, **11**, 957 (2000).
54) Morigami, Y., Kondo, M., Abe, J., Kita, H., Okamoto, K., *Separ. Purif. Technol.*, **25**, 251 (2001).
55) Bowen, T. C., Noble, R. D., Falconer, J. L., *J. Membr. Sci.*, **245**, 1 (2004).
56) Tojo, M., Fukuoka, Y., Jpn. Tokkyo Koho, 03-002014 (1991).

……

要　　旨

ナノサイズゼオライトの合成法とゼオライト膜への展開

多湖　輝興，中坂　佑太，増田　隆夫

北海道大学大学院工学研究院有機プロセス工学部門化学工学分野，060-8628 札幌市北区北13条西8丁目

固体酸性と分子ふるい能を併せ持つゼオライトは，反応プロセスや分離プロセスにおける重要な物質である。さらに，膜形状のゼオライトは，無機膜の特性（耐熱，耐薬品性）とゼオライトの特性を併せ持つ。そのため，ゼオライト膜は，分離膜，反応膜，および反応分離膜としての応用が期待され，多くの研究者に注目されてきた。ゼオライト膜の特性を十分に引き出すためには，その基材となるゼオライトの結晶サイズ制御，およびゼオライト膜における酸点の位置選択的不活性化と細孔経の制御が有効である。本稿では，エマルション法によるナノサイズゼオライト合成法と有機シラン化合物を用いたゼオライト酸点の位置選択的な不活性化法（CCS 法）を紹介する。そして，ゼオライトの結晶サイズと CCS 処理がゼオライト膜特性に及ぼす影響について概説する。

……